Check for updates

Diabetes, Obesity and Metabolism

WILEY

ORIGINAL ARTICLE OPEN ACCESS

Nephroprotective Effects of the Dual GCGR/GLP-1R Agonist Survodutide in Hypertension-Accelerated Diabetic Kidney Disease

Alexander Hamilton[1] | Louise Thisted[1] | Maria Ougaard[1] | Max Hahn[1] | Kasper Andersen[1] | Johanna Perens[1] | Robert Augustin[2] | Besnik Bajrami[2] | Wolfgang Rist[2] | Michael Christensen[1] | Henrik H. Hansen[1] | Thomas Klein[2]

[1]Gubra A/S, Hørsholm, Denmark | [2]Boehringer Ingelheim Pharma GmbH & Co. KG, Biberach an der Riss, Germany

Correspondence: Thomas Klein (thomas_1.klein@boehringer-ingelheim.com) | Henrik H. Hansen (hbh@gubra.dk)

Received: 8 May 2026 | **Revised:** 4 September 2026 | **Accepted:** 16 September 2026

Handling Editor: Nigel Irwin

Keywords: diabetic kidney disease | dual agonist | glucagon receptor | glucagon-like peptide-1 receptor | obesity | oxyntomodulin analogue | survodutide

ABSTRACT

Aims: Survodutide is a novel long-acting dual glucagon (GCGR)/glucagon-like peptide-1 (GLP-1R) receptor agonist currently in phase-3 clinical development for the treatment of people living with obesity and metabolic dysfunction-associated steatohepatitis. Emerging evidence suggests impaired renal GCGR function in chronic kidney disease (CKD), including diabetic kidney disease (DKD). This study aimed to characterize the effects of survodutide in a translational mouse model of advanced DKD, induced by adeno-associated virus-mediated renin overexpression (ReninAAV) in uninephrectomized (UNx) diabetic *db/db* mice.

Materials and Methods: Female obese and diabetic *db/db* C57BKS mice received a single intravenous dose of ReninAAV 1 week prior to UNx. Three weeks post-UNx, *db/db* UNx-ReninAAV mice were administered (s.c., q.d.) vehicle or survodutide (7.5 nmol/kg) for 10 weeks. Endpoints included blood/urine biochemistry, histological markers of glomerulosclerosis, tubular injury and inflammation, as well as quantitative 3D whole-pancreas and whole-kidney imaging.

Results: Compared to vehicle controls, survodutide reduced body weight, hyperglycemia, and HbA1c levels concurrent with improved hyperinsulinemia and β-cell islet volume distribution. Notably, survodutide promoted substantial benefits on advanced albuminuria, severe glomerulosclerosis, kidney hypertrophy and inflammation. 3D whole-kidney imaging revealed that survodutide significantly reduced kidney and glomerular hypertrophy while increasing glomerular density and improving glomerular sphericity. Survodutide reduced liver weight and plasma amino acid levels, including alanine, confirming hepatic glucagon receptor activation.

Conclusions: Survodutide markedly improved metabolic and renal outcomes in the *db/db* UNx-ReninAAV mouse model of advanced DKD, supporting further investigation into therapeutic options of survodutide in chronic kidney diseases.

Abbreviations: β2M, beta-2-microglobulin; 3-HB, 3-hydroxybutyrate (β-hydroxybutyrate); AAV, adeno-associated virus; ACE, angiotensin-converting enzyme; ACR, albumin-to-creatinine ratio; CKD, chronic kidney disease; *db/db*, leptin receptor-deficient diabetic mouse model; DKD, diabetic kidney disease; EC50, half maximal effective concentration; eGFR, estimated glomerular filtration rate; ESKD, end-stage kidney disease; GCGR, glucagon receptor; GLP-1, glucagon-like peptide-1; GLP-1R, glucagon-like peptide-1 receptor; HbA1c, glycated haemoglobin A1c; KIM-1, kidney injury molecule-1; LC–MS/MS, liquid chromatography–tandem mass spectrometry; LCS SPIM, large Cleared Samples Selective Plane Illumination Microscopy; MCP-1, monocyte chemoattractant protein-1; NGAL, neutrophil gelatinase-associated lipocalin; OPN, osteopontin; PAS, Periodic acid-Schiff; QD, once daily (quaque die); Ren1d, mouse renin 1d gene; SC, subcutaneous; SGLT2, sodium-glucose cotransporter 2; uACR, urine albumin-to-creatinine ratio; UNx, uninephrectomy.

This is an open access article under the terms of the Creative Commons Attribution-NonCommercial-NoDerivs License, which permits use and distribution in any medium, provided the original work is properly cited, the use is non-commercial and no modifications or adaptations are made.

© 2026 The Author(s). *Diabetes, Obesity and Metabolism* published by John Wiley & Sons Ltd.

1 | Introduction

Diabetes and hypertension together contribute to more than 60% of end-stage kidney disease (ESKD) cases worldwide, making them the leading causes of chronic kidney disease (CKD) globally [1]. Among these, type 2 diabetes alone accounts for an estimated 30%–50% of CKD and ESKD cases, substantially heightening the risk of cardiovascular events, premature mortality and escalating healthcare costs [2, 3]. As the prevalence of diabetic kidney disease (DKD) continues to rise, it represents a growing global health burden and a critical challenge for healthcare systems.

DKD is clinically characterized by a progressive decline in renal function. While hyperglycemia is a primary driver, several metabolic risk factors, including hypertension, obesity and dyslipidemia, also contribute significantly to DKD pathogenesis [4]. Accordingly, DKD management focuses on optimizing glycemic control, slowing kidney function decline and mitigating cardiovascular risk. For decades, the cornerstone of DKD management has involved lifestyle modification alongside pharmacologic blockade of the renin-angiotensin system, primarily through the use of angiotensin-converting enzyme (ACE) inhibitors or angiotensin II receptor blockers [5]. Sodium–glucose cotransporter 2 (SGLT2) inhibitors have have also become valuable adjuncts in DKD management More recently, glucagon-like peptide-1 receptor (GLP-1R) agonists have emerged as a distinct drug class with additional kidney protective benefits. Beyond their glucose-lowering effects, GLP-1R agonists provide renoprotective, cardioprotective and anti-inflammatory benefits, supported by robust clinical trial evidence [6–11].

Emerging evidence suggests a functional role for glucagon receptor (GCGR) signalling in renal physiology. GCGRs are highly expressed in the kidney, especially in the thick ascending loop of Henle and distal tubules [12, 13]. Notably, GCGR expression is downregulated in CKD [14, 15] and positively correlates with the estimated glomerular filtration rate (eGFR) in patients with DKD [16]. Supporting a functional role for renal GCGR signalling, mice with kidney-specific *Gcgr* deletion develop chronic kidney disease characterized by pronounced albuminuria, hypertension and electrolyte imbalances [17]. While direct clinical evidence of GCGR-mediated renoprotective effects is still emerging [18], these findings suggest that targeting GCGR, particularly in combination with GLP-1R agonism, may offer added therapeutic benefit in the management of DKD.

Survodutide is a novel long-acting GCGR/GLP-1R dual agonist [19], currently in phase-3 clinical development for the treatment of people living with obesity (SYNCHRONIZE trials) and those living with metabolic dysfunction-associated steatohepatitis (LIVERAGE trials) [20, 21]. Given its combined activation of GCGR and GLP-1R signalling, we evaluated the efficacy of survodutide in a translational mouse model of advanced DKD, induced by adeno-associated virus (AAV)–mediated renin overexpression in uninephrectomized (UNx) diabetic *db/db* mice [22, 23].

2 | Materials and Methods

2.1 | Animals

The study was approved by The Danish Animal Experiments Inspectorate (license 2023-15-0201-01456). Female *db/db* (BKS.Cg-Dock7m+/+Leprdb/J) mice (Charles River, Calco, Italy) arrived at 5–6 weeks of age and were group-housed in a controlled environment (12 h light/dark cycle, 24°C ± 2°C, humidity 50% ± 10%). Female *db/db* mice are less susceptible to developing age-related hydronephrosis and pyelonephritis than male *db/db* mice [24–26], and were therefore used in the present study. Animals had access to plenty of bedding material, shelters and chewing sticks. Mice had ad libitum access to tap water and chow (Altromin 1324, 3.2 kcal/kg, 11 kcal-% fat, 24 kcal-% protein, 65 kcal-% carbohydrate, Brogaarden, Denmark).

2.2 | Drug Treatment

See study outline in Figure 1A. In brief, *db/db* mice (8–9 weeks) were intravenously injected via the tail vein with an adeno-associated virus (AAV) vector encoding the mouse *Ren1d* gene (AAV8-TBG-m-Ren1d, Vector Biolabs) (1.5×10^{10} Genome Copies, GC, Week-4) and underwent UNx (Week-3) 67 days later, from this point to study end mice were single-housed. One week before treatment start (Week-1), *db/db* UNx-ReninAAV mice were randomized into experimental groups based on body weight, urine albumin-to-creatinine ratio (uACR), and fed blood glucose. Mice received (SC, QD) of vehicle (50 mM phosphate buffer pH 7.0 + 5% mannitol) or survodutide (7.5 nmol/kg) for 10 weeks ($n = 15$ per group) [22, 27]. Human translational dose-prediction analysis indicated that this survodutide dose in mice corresponds to an approximately 4.5 to 8.0 mg once-weekly subcutaneous dose in humans (Figure S2), supporting the clinical relevance and translational rationale for the selected dose.

2.3 | Plasma and Urine Biochemistry

Blood and urine samples were collected every 2 weeks from non-fasted animals for glucose monitoring. Terminal blood samples were analysed for blood glucose and glycated haemoglobin A1c (HbA1c) as well as plasma insulin, urea, cystatin C [22, 25]. Spot urine samples were assayed for glucose, albumin, creatinine, cystatin C, urea and kidney injury molecule-1 (KIM-1) [22, 25]. Urine albumin-to-creatinine ratio (uACR) was calculated. Plasma renin, cystatin C and kidney injury molecule-1 (KIM-1) were determined using ELISA (R&D Systems). Plasma 3-hydroxybutyrate (3-HB, β-hydroxybutyrate) levels were determined using an enzyme-based colorimetric assay (#MAK540, Sigma-Aldrich). HbA1c was measured using a commercial kit (Roche Diagnostics) using a Cobas c501 autoanalyser. Plasma amino acids were determined using LC–MS/MS analysis [19]. Plasma albumin, β2-microglobulin (β2M), calbindin, clusterin, monocyte chemoattractant protein-1 (MCP-1), neutrophil gelatinase-associated lipocalin (NGAL) and osteopontin biomarkers were assayed using a mouse/rat multiplex assay (Ampersand Biomedicine, Lake Clean, NY). *db/db*

14631326, 2026, 12, Downloaded from https://dom-pubs.onlinelibrary.wiley.com/doi/10.1111/dom.71387, Wiley Online Library on [05/11/2026]. See the Terms and Conditions (https://onlinelibrary.wiley.com/terms-and-conditions) on Wiley Online Library for rules of use; OA articles are governed by the applicable Creative Commons License

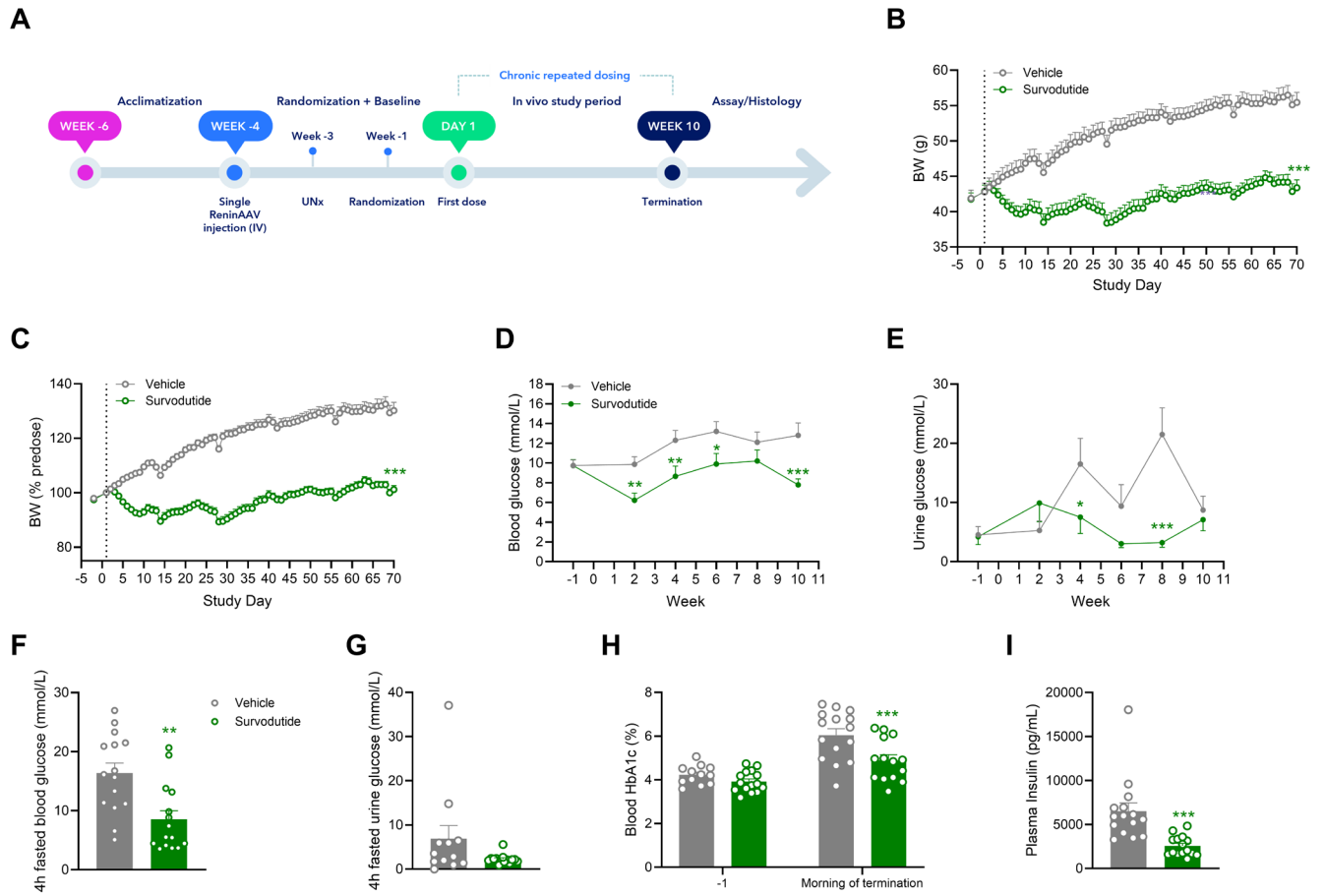


FIGURE 1 | Survodutide suppresses weight gain and improves glycemia in *db/db* UNx-ReninAAV mice. (A) Study outline. (B, C) Absolute (g) and relative (% vs. baseline) body weight profiles ($n = 15$ mice per group). (D) Fed blood glucose (mmol/L) profiles (14–15 samples per time point). (E) Fed urine glucose (mmol/L) profiles (9–14 samples per time point). (F) 4 h fasted blood glucose at Week 9 ($n = 15$ mice per group). (G) 4 h fasted urine glucose at Week 9 ($n = 12$–14 samples per group). (H) Blood HbA1c at Week-1 and Week 10 ($n = 12$–15 samples per group). (I) Plasma Insulin at Week 10 ($n = 15$ samples per group). Data presented as mean ± SEM. For body weight measurements statistics were only performed at termination. For single timepoint data, Dunnett's test one-factor linear model used. For data with multiple timepoints, Dunnett's test on two-factor linear model with interaction used. *$p < 0.05$, **$p < 0.01$, ***$p < 0.001$ compared to the Vehicle group.

UNx-ReninAAV mice exhibit glomerular hyperfiltration rather than a decline in GFR [22], GFR was therefore not assessed in the present study.

2.4 | 2D Histological Analyses

F4/80 and KIM-1 stained sections were scanned with a 20× objective and quantified in whole-kidney sections, expressed as proportional (%) surface area of immunopositive staining [25, 27, 28]. Glomerulosclerosis scoring was performed on Periodic acid-Schiff (PAS) stained sections by AI-assisted image analysis [22].

2.5 | 3D Whole-Organ Imaging Analysis

Fixed kidneys and pancreata were cleared and stained for podocin and insulin, respectively, optically cleared and imaged using a Bruker Luxendo LCS SPIM microscope with dual-sided illumination (4.4× objective; 10 µm z-steps, 6.3 µm beam expander). Autofluorescence and target signal were measured in multiple-tile acquisition at 488/642 nm (kidney) and 561/642 nm (pancreata). Volumetric datasets were processed and then analysed using automated 3D segmentation algorithms to quantify kidney glomeruli (volume, count, density, sphericity) and pancreatic b-cells (volume, count, density, size distribution), all of which were normalized to total tissue volume. A detailed description of the 3D imaging analysis can be found in the Supporting Information.

2.6 | Statistics

For single-timepoint data, a one-factor linear regression model with the treatment groups as categorical, independent (predictor) variables was applied, Dunnett's test compared treatments to control. For repeated or multi-category data, a two-factor linear regression model with the treatment groups and time points as categorical independent (predictor) variables with interaction was used. Dunnett's test was used to compare treatment groups with the respective control at each time point. Plasma amino acid levels were analysed using an unpaired *t*-test. Coefficients of variation (CVs) are reported where appropriate.

14631326, 2026, 12, Downloaded from https://dom-pubs.onlinelibrary.wiley.com/doi/10.1111/dom.71387, Wiley Online Library on [05/11/2026]. See the Terms and Conditions (https://onlinelibrary.wiley.com/terms-and-conditions) on Wiley Online Library for rules of use; OA articles are governed by the applicable Creative Commons License

3 | Results

At Week-1, *db/db* UNx-ReninAAV mice were randomized and stratified into groups based on urine albumin-to-creatinine ratio (uACR), body weight and fed blood glucose levels (Figure S1). Vehicle-dosed *db/db* UNx-ReninAAV mice exhibited continuous weight gain throughout (Figure 1B,C), reflecting the characteristic hyperphagic phenotype of *db/db* mice. In contrast, once-daily administration of survodutide initially led to mild weight loss, followed by a gradual return to baseline body weight. At termination, body weight in the survodutide-treated group was markedly and significantly lower compared to the vehicle group, both in terms of absolute (vehicle: 55.5 ± 1.4 g vs. survodutide: 43.5 ± 1.1 g, $p \leq 0.001$; Figure 1B,C) and relative measurements compared to baseline (vehicle: 130% ± 3.0% vs. survodutide: 101% ± 1.5%, $p \leq 0.001$; Figure 1B,C).

In addition to its suppression of weight gain, survodutide significantly improved hyperglycemia at Weeks 2, 4, 6 and 10 compared to the vehicle group (Figure 1D). Correspondingly, fed urine glucose was also improved by survodutide administration with significantly lower levels at Week 4 and Week 8 (Figure 1E). Additionally, 4 h fasted blood glucose levels measured at Week 9 were significantly lower in the survodutide-treated group relative to vehicle controls (vehicle: 16.5 ± 1.7 mmol/L vs. survodutide: 8.3 ± 1.5 mmol/L, $p = 0.002$; Figure 1F). 4 h fasted urine glucose measured at Week 9 was also substantially lower compared to vehicle; however, this reduction did not reach statistical significance (vehicle: 6.9 ± 3.0 mmol/L vs. survodutide: 2.3 ± 0.3 mmol/L, $p = 0.108$; Figure 1G). Blood HbA1c, a measure of long-term average blood glucose levels, was measured at Week-1 and Week 10 (prior to termination). While baseline levels were similar between vehicle and survodutide groups (Figure 1H), 10 weeks of survodutide treatment caused a significant ~20% reduction in blood HbA1c compared to vehicle (vehicle: 6.1% ± 0.3% vs. survodutide: 4.9% ± 0.3%, $p \leq 0.001$; Figure 1H). Plasma insulin levels measured at Week 10 were ~60% reduced in the survodutide treated group relative to the vehicle group (vehicle: 6.5 ± 0.9 pg/mL vs. survodutide: 2.6 ± 0.3 pg/mL, $p \leq 0.001$; Figure 1I).

In analyses of kidney function, uACR increased progressively in vehicle-dosed *db/db* UNx-ReninAAV mice, indicative of advancing diabetic nephropathy. Notably, survodutide administration kept uACR stable throughout the study duration with significantly lower levels at Weeks 4, 6, 8 and 10 compared to vehicle (Figure 2A). When analysed separately, urine albumin was reduced by survodutide treatment with significant reductions at Weeks 6, 8 and 10 (Figure 2B) while urine creatinine increased, with significant elevation at Weeks 4 and 10 (Figure 2C). Plasma renin, which measures the functionality

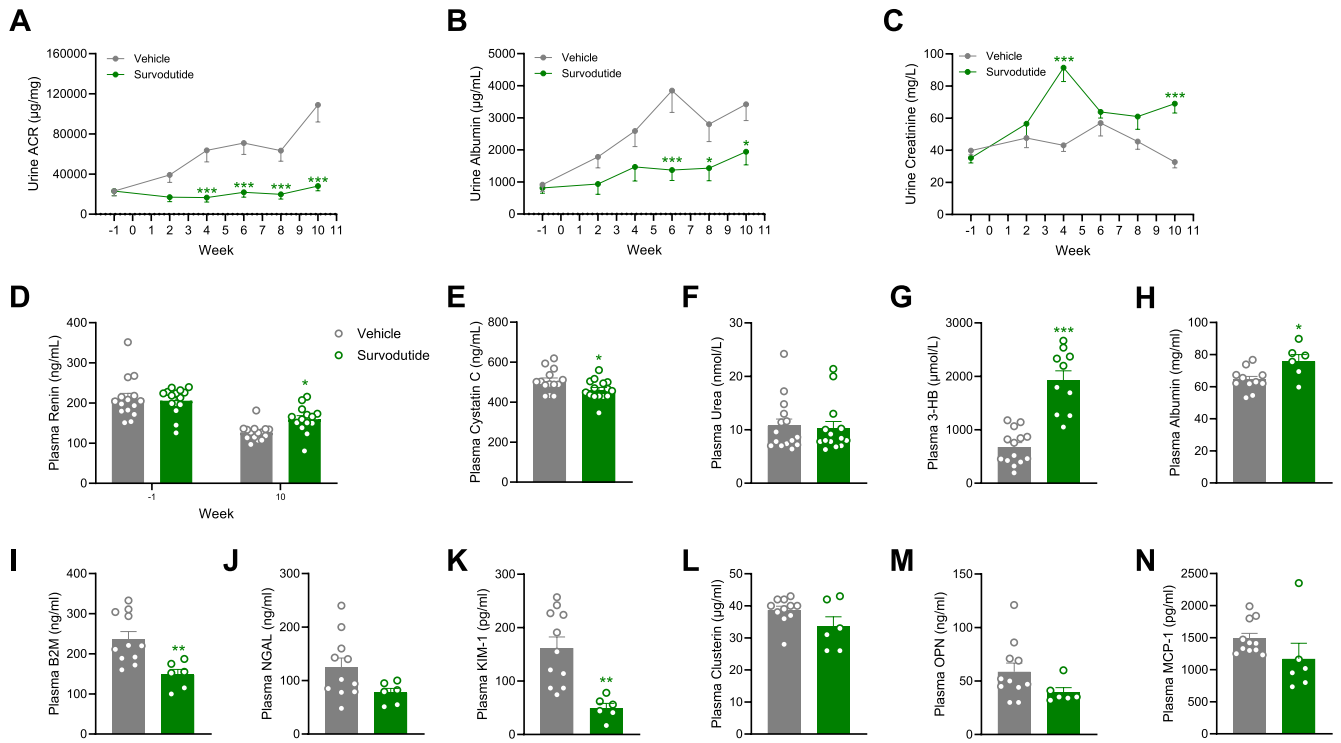


FIGURE 2 | Survodutide improves biomarkers of kidney function in *db/db* UNx-ReninAAV mice. Profiles of urine (A) albumin-creatinine ratio (uACR, µg/mg), (B) albumin (µg/mL) and (C) creatinine (mg/L). $n = 13–15$ samples per time point for uACR, urine albumin and creatine measurements. (D) Plasma renin levels (ng/mL) at Week-1 and Week 10. Plasma levels of (E) Cystatin C (ng/mL), (F) urea (nmol/L). $n = 14–15$ for plasma renin, cystatin C and urea measurements. (G) 3-hydroxybutyric acid (3-HB, µmol/L), all at Week 10 ($n = 10–14$ per group). (H) Plasma levels of albumin (mg/mL, $n = 6–10$ per group), (I) Beta-2 microglobulin (B2M, ng/mL), (J) neutrophil gelatinase-associated lipocalin (NGAL, ng/mL), (K) kidney injury molecule (KIM-1, pg/mL), (L) clusterin (µg/mL), osteopontin (OPN, ng/mL) and (N) monocyte chemoattractant protein-1 (MCP-1, pg/mL). $n = 6–11$ per group for B2M, NGAL, KIM-1, clusterin, OPN and MCP-1 measurements. Data presented as mean ± SEM. For single timepoint data, Dunnett's test one-factor linear model used. For data with multiple timepoints, Dunnett's test on two-factor linear model with interaction used. $^*p < 0.05$, $^{**}p < 0.01$, $^{***}p < 0.001$ compared to the Vehicle group.

14631326, 2026, 12, Downloaded from https://dom-pubs.onlinelibrary.wiley.com/doi/10.1111/dom.71387, Wiley Online Library on [05/11/2026]. See the Terms and Conditions (https://onlinelibrary.wiley.com/terms-and-conditions) on Wiley Online Library for rules of use; OA articles are governed by the applicable Creative Commons License

of the kidney renin-angiotensin-aldosterone system, was evaluated at Week-1 and Week 10. Renin levels were significantly higher in the survodutide- vs. vehicle-treated group at Week 10 (vehicle: 126 ± 5.0 ng/mL vs. survodutide: 160 ± 9.0 ng/mL, $p = 0.016$; Figure 2D). Plasma cystatin C, a biomarker for glomerular filtration which increases with the progression diabetic nephropathy [29] was reduced by survodutide administration at Week 10 relative to vehicle (vehicle: 505 ± 16 ng/mL vs. survodutide: 461 ± 50 ng/mL, $p = 0.035$; Figure 2E). There was no difference in plasma urea between the groups at Week 10 (vehicle: 10.7 ± 1.3 nmol/L vs. survodutide: 10.3 ± 1.3 nmol/L, $p = 0.796$; Figure 2F). Survodutide markedly reduced liver weight (vehicle: 2.5 ± 0.2 g vs. survodutide: 1.3 ± 0.1 g, $p \leq 0.001$; Figure S3). Plasma 3-HB concentrations, a key biomarker of hepatic ketogenesis and fatty acid oxidation, were increased by survodutide at Week 10 (vehicle: 675 ± 86 μmol/L vs. survodutide: 1918 ± 184 μmol/L, $p \leq 0.001$; Figure 2G) and reduced plasma amino acid levels (Figure S4), reflecting that survodutide enhanced hepatic glucagon signalling, indicative of target engagement. Further measurements of plasma biomarkers showed increased plasma albumin levels following survodutide treatment (vehicle: 64.3 ± 21 mg/mL vs. survodutide: 75.8 ± 42 mg/mL, $p < 0.05$, Figure 2H), consistent with the observed reduction in urinary albumin excretion. Plasma β2M levels were significantly reduced by survodutide (vehicle: 237 ± 19 ng/mL vs. survodutide: 147 ± 14 ng/mL, $p < 0.01$; Figure 2I), suggesting improved glomerular filtration. Plasma NGAL, a marker of acute kidney injury, was also reduced after survodutide treatment, although this change did not reach statistical significance (vehicle: 124 ± 18 ng/mL vs. survodutide: 77.0 ± 8.3 ng/mL, $p = 0.08$; Figure 2J). In contrast, plasma KIM-1 levels, a marker of kidney damage, declined markedly following survodutide treatment (vehicle: 162 ± 21 pg/mL vs. survodutide: 49.7 ± 8.5 pg/mL, $p < 0.01$, Figure 2K). Levels of plasma clusterin (vehicle: 36.6 ± 1.3 μg/mL vs. survodutide: 33.3 ± 3.1 μg/mL, $p = 0.08$, Figure 2L), osteopontin (OPN; vehicle: 58.6 ± 8.1 ng/mL vs. survodutide: 39.5 ± 4.3 ng/mL, $p = 0.12$, Figure 2M) and MCP-1 (vehicle: 1486 ± 80 pg/mL vs. survodutide: 1169 ± 244 pg/mL, $p = 0.15$, Figure 2N), systemic inflammatory markers that are often elevated in kidney disease, were also reduced by survodutide, but these effects did not attain statistical significance. Further evaluation of kidney health using histology supported the nephroprotective effect of survodutide in *db/db* UNx-ReninAAV mice. Using PAS staining to highlight kidney structure revealed robustly reduced glomerulosclerosis severity in survodutide-treated mice compared to vehicle (Figure 3A), as demonstrated by overall lowered glomerulosclerosis scores (Figure 3B), a significantly lower glomerulosclerosis index (Vehicle: 0.78 ± 0.09 vs. survodutide: 0.3 ± 0.05, $p \leq 0.001$; Figure 3C) and a significantly reduced proportion of glomeruli with advanced or severe glomerulosclerosis (G3 + G4 fraction, vehicle: 13.7% ± 2.4% vs. survodutide: 3.3% ± 0.9%, $p \leq 0.001$; Figure 3D). Staining with F4/80, a marker for macrophages, revealed extensive macrophage infiltration in the vehicle-treated group which was reduced in the survodutide group (Figure 3E) with significant reductions at both total (vehicle: 11.4 ± 1.3 mg vs. survodutide: 5.18 ± 0.3 mg, $p \leq 0.001$; Figure 3F) and relative (%-area) levels (vehicle: 4.11% ± 0.5% vs. survodutide: 2.13% ± 0.2%, $p \leq 0.001$; Figure 3G). Immunostaining for KIM-1 suggested reduced levels after survodutide treatment when assessed visually (Figure 3H), however, the effect did not attain statistical significance against vehicle at both total (vehicle: 3.64 ± 0.87 mg vs. survodutide: 2.10 ± 0.6 mg, $p = 0.141$; Figure 3I) and relative levels (vehicle: 1.29% ± 0.28% vs. survodutide: 0.92% ± 0.28%, $p = 0.363$; Figure 3J).

Quantitative 3D imaging was used to assess whole-organ histomorphometric changes induced by survodutide in the kidney and pancreas of *db/db* UNx-ReninAAV mice. There was a clear change in glomeruli morphology after survodutide treatment, as visualized by podocin-1 staining (Figure 4A). Kidney volume was reduced in the survodutide treatment group compared to vehicle (vehicle: 214 ± 4.5 mm^3, CV = 7.9%, $n = 14$ vs. survodutide: 181 ± 23.6 mm^3, CV = 13.0%, $n = 15$, $p \leq 0.001$; Figure 4C), in line with reduced total kidney weight (vehicle: 0.28 ± 0.01 g vs. survodutide: 0.25 ± 0.01 g, $p = 0.0107$; Figure 4D). Notably, the total 3D quantified glomeruli volume was significantly reduced in the survodutide-treated group (vehicle: 6.23 ± 0.20 mm^3, CV = 12.1%, $n = 14$ vs. survodutide: 5.34 ± 0.25 mm^3, CV = 17.9%, $n = 15$, $p = 0.0104$; Figure 4E) while glomerular volume fraction (vehicle: 2.91% ± 0.078%, CV = 10.1%, $n = 14$ vs. survodutide: 2.96% ± 0.12%, CV = 15.7%, $n = 15$, $p = 0.723$, Figure 4F) and total counts (vehicle: 14452 ± 396, CV = 10.3%, $n = 14$ vs. survodutide: 13981 ± 192, CV = 5.3%, $n = 15$, $p = 0.285$, Figure 4G) were unchanged, suggesting a reduction in glomerular hypertrophy without an alteration in glomerular number. Correspondingly, survodutide increased glomerular density (Vehicle: 67.7 ± 1.8 per mm^3, CV = 10.0%, $n = 14$ vs. survodutide: 78.3 ± 2.7 per mm^3, CV = 13.4%, $n = 15$, $p = 0.003$; Figure 4H) while slightly reducing individual mean glomerular volume (vehicle: 0.432 ± 0.010 μm^3, CV = 8.9%, $n = 14$ vs. survodutide: 0.381 ± 0.015 μm^3, CV = 15.6%, $n = 15$, $p \leq 0.012$; Figure 4I). To further quantitatively assess changes in glomeruli morphology, we measured glomerular sphericity, a marker of glomerular morphological integrity [30, 31]. Glomeruli sphericity (more round glomeruli) was significantly increased following survodutide treatment (vehicle: 0.81 ± 0.004, CV = 1.98%, $n = 14$ vs. survodutide: 0.83 ± 0.002, CV = 0.9%, $n = 15$, $p < 0.001$; Figures 4J and S5). Mean glomerular podocin fluorescence intensity was unchanged by survodutide treatment (data not shown).

In the pancreas, there were no clear visual differences in total volume of the pancreas and total volume of insulin-positive ($insulin^+$) islets between vehicle and survodutide (Figure 5A). Accordingly, survodutide had no effect on pancreas volume (vehicle: 105 ± 5.0 mm^3, CV = 17.3%, $n = 13$ vs. survodutide: 103 ± 4.5 mm^3, CV = 15.9%, $n = 13$, $p = 0.68$; Figure 5B) or $insulin^+$ cell volume, both in terms of absolute volume (vehicle: 0.99 ± 0.13 mm^3, CV = 45.8%, $n = 13$ vs. survodutide: 1.20 ± 0.19 mm^3, CV = 57.2%, $n = 13$, $p = 0.365$; Figure 5C) and when normalized to pancreas volume (vehicle: 0.96% ± 0.15%, CV = 55.36%, $n = 13$ vs. survodutide: 1.24% ± 0.23%, CV = 65.6%, $n = 13$, $p = 0.295$; Figure 5D). Furthermore, there was no difference in the total number of $insulin^+$ islets (islets containing insulin signal) between the two groups (vehicle: 2730 ± 167, CV = 22.0%, $n = 13$ vs. survodutide: 2490 ± 198, CV = 28.7%, $n = 13$, $p = 0.357$; Figure 5E), nor in the islet density (vehicle: 26.2 ± 1.5 per mm^3, CV = 19.9%, $n = 13$ vs. survodutide: 24.8 ± 2.2 per mm^3, CV = 32.5%, $n = 13$, $p = 0.613$; Figure 5F). Stratification

14631326, 2026, 12, Downloaded from https://dom-pubs.onlinelibrary.wiley.com/doi/10.1111/dom.71387, Wiley Online Library on [05/11/2026]. See the Terms and Conditions (https://onlinelibrary.wiley.com/terms-and-conditions) on Wiley Online Library for rules of use; OA articles are governed by the applicable Creative Commons License

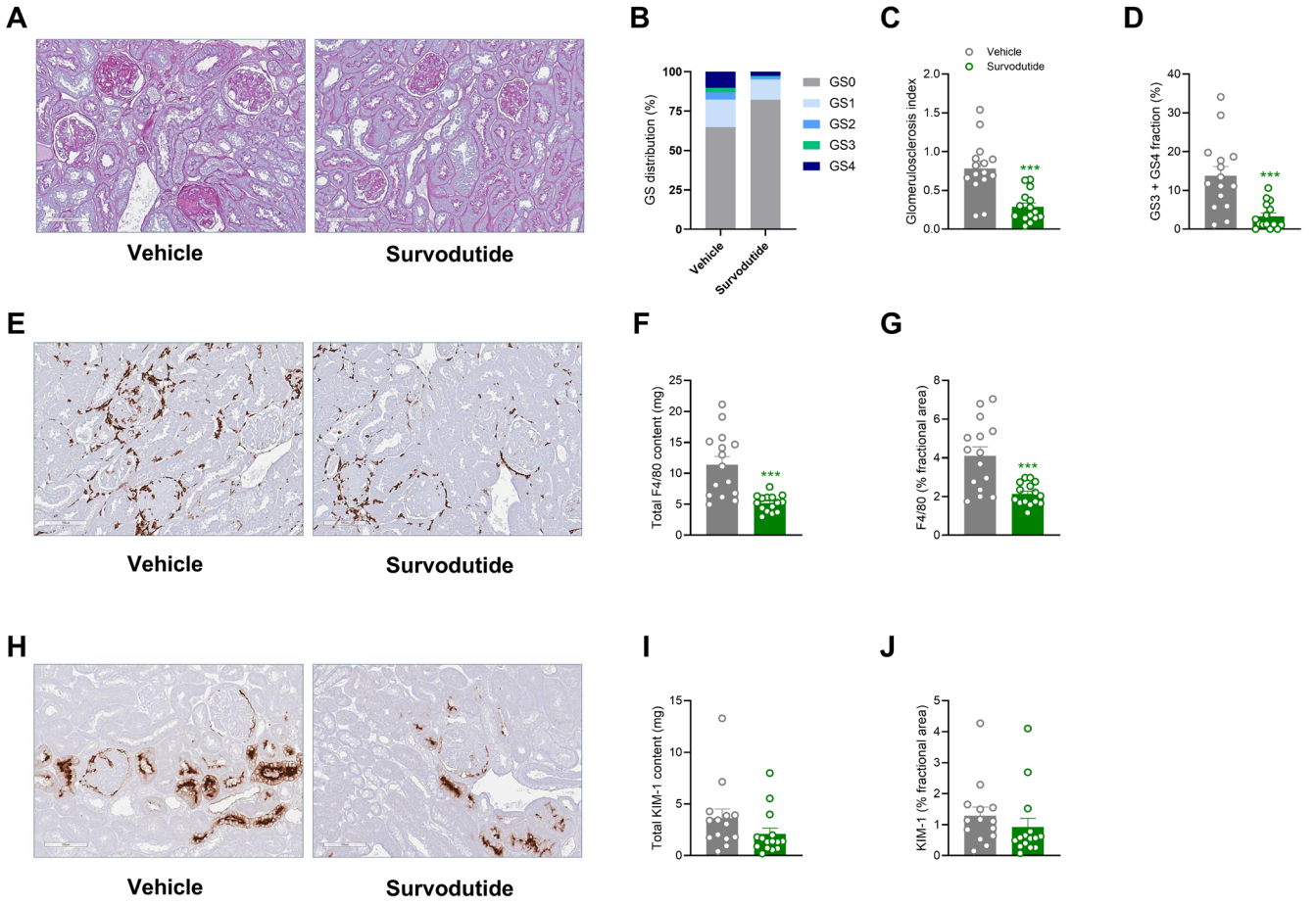


FIGURE 3 | Survodutide reduces glomerulosclerosis and kidney macrophage infiltration in *db/db* UNx-ReninAAV mice. (A) Representative images of PAS-stained kidney sections in vehicle (left panel) and survodutide (right panel) groups (magnification, 20×, scale bar, 100 μm). (B) Distribution of glomerulosclerosis score (GS) based on a 5-point scale according to sclerotic area: GS0 (normal), GS1 (mild, sclerotic area up to 25%), GS2 (moderate, sclerotic area of 25%–50%), GS3 (severe, sclerotic area of 51%–75%) and GS4 (global, sclerotic area of 76%–100%). (C) Mean glomerulosclerosis score (glomerulosclerosis index). (D) Relative proportion (%) of severe sclerotic glomeruli (GS3 + GS4 fraction). (E) Representative images of F4/80-stained kidney sections in vehicle (left panel) and survodutide (right panel) groups (magnification, 20×, scale bar, 100 μm). (F, G) Total (mg) and relative (% fractional area) levels of F4/80. (H) Representative images of KIM-1-stained kidney sections in vehicle (left panel) and survodutide (right panel) groups (magnification, 20×, scale bar, 100 μm). (I, J) Total (mg) and relative (% fractional area) of KIM-1. Data presented as mean ± SEM ($n = 15$ per group). Dunnett's test one-factor linear model used. ***$p < 0.001$ compared to the Vehicle group.

of pancreatic islets by size revealed that, in the survodutide-treated group, larger islets contributed a greater proportion of total insulin$^+$ islet volume compared to vehicle controls, particularly among mid-sized islets (at 0.0096 and 0.0192 mm^3, $p = 0.00654$ and $p = 0.00405$, Figure 5G). However, the number of insulin-positive islets across all size categories remained unchanged (Figure 5H).

4 | Discussion

Survodutide, a long-acting dual GCGR/GLP-1R agonist, demonstrated robust renoprotective efficacy after 10 weeks of subcutaneous treatment at a clinically relevant dose in the translational *db/db* UNx-ReninAAV mouse model of hypertension-accelerated DKD. Survodutide prevented the progression of albuminuria, improved markers of kidney injury and glomerular filtration, and markedly ameliorated histopathological features of advanced glomerulosclerosis and renal inflammation. These benefits were accompanied by reduced kidney volume and improved glomerular structural integrity, characterized by reduced hypertrophy and restored sphericity. Collectively, these preclinical findings demonstrate broad renoprotective efficacy of survodutide across multiple key hallmarks of DKD.

In parallel with its renal effect, survodutide significantly improved metabolic parameters, including body weight, hyperglycemia, hyperinsulinemia and hepatomegaly. These findings are consistent with previous reports of survodutide efficacy in diabetic *db/db* mice [32]. Body weight gradually returned towards baseline in survodutide-treated *db/db* UNx-ReninAAV mice. However, given the marked hyperphagia and progressive weight gain characteristic of *db/db* mice, the effects of weight-lowering interventions in this model may primarily manifest as attenuation of progressive weight gain rather than sustained weight loss relative to baseline [33]. Furthermore, the present study provides evidence of GCGR engagement by survodutide, as indicated by elevated plasma 3-HB levels and reduced plasma amino acid concentrations.

14631326, 2026, 12, Downloaded from https://dom-pubs.onlinelibrary.wiley.com/doi/10.1111/dom.71387, Wiley Online Library on [05/11/2026]. See the Terms and Conditions (https://onlinelibrary.wiley.com/terms-and-conditions) on Wiley Online Library for rules of use; OA articles are governed by the applicable Creative Commons License

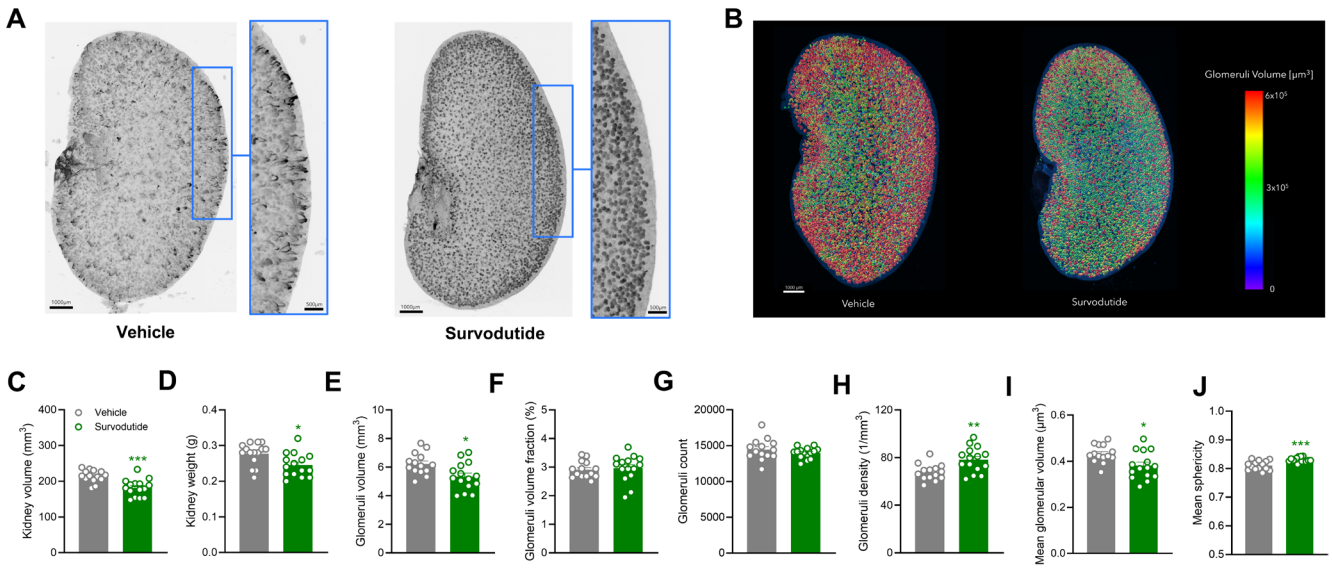


FIGURE 4 | Survodutide reduces kidney and glomerular volumes in *db/db* UNx-ReninAAV mice, as quantified by 3D whole-kidney light-sheet fluorescence microscopy. (A) Representative maximum intensity projections show podocin staining in whole kidneys, after tissue clearing and acquired by volumetric 3D light sheet fluorescence microscope (LSFM) imaging. Magnified views are outlined in blue, displaying clear morphological differences at nephron-glomeruli networks. Scale bar, 1000 µm; zoomed-in scale bar, 500 µm. (B) Representative images displaying glomeruli segmentation, each coloured sphere represents a single glomerulus, the colour of which represents glomerular volume—based on the key on the right. Note, the clear reduction in glomeruli size after survodutide treatment. Graphs display (C) total kidney volume (mm^3), (D) kidney weight (g), (E) glomeruli volume (mm^3), (F) glomeruli volume fraction (%, normalized to total kidney volume), (G) glomeruli count, (H) glomeruli density (glomeruli/mm^3, normalized to total kidney volume) and (I) mean individual glomerular volume (mm^3). (J) mean glomerular sphericity. Data presented as mean ± SEM ($n = 14–15$ per group). Dunnett's test one-factor linear model used. *$p < 0.05$, **$p < 0.01$, ***$p < 0.001$ compared to the Vehicle group.

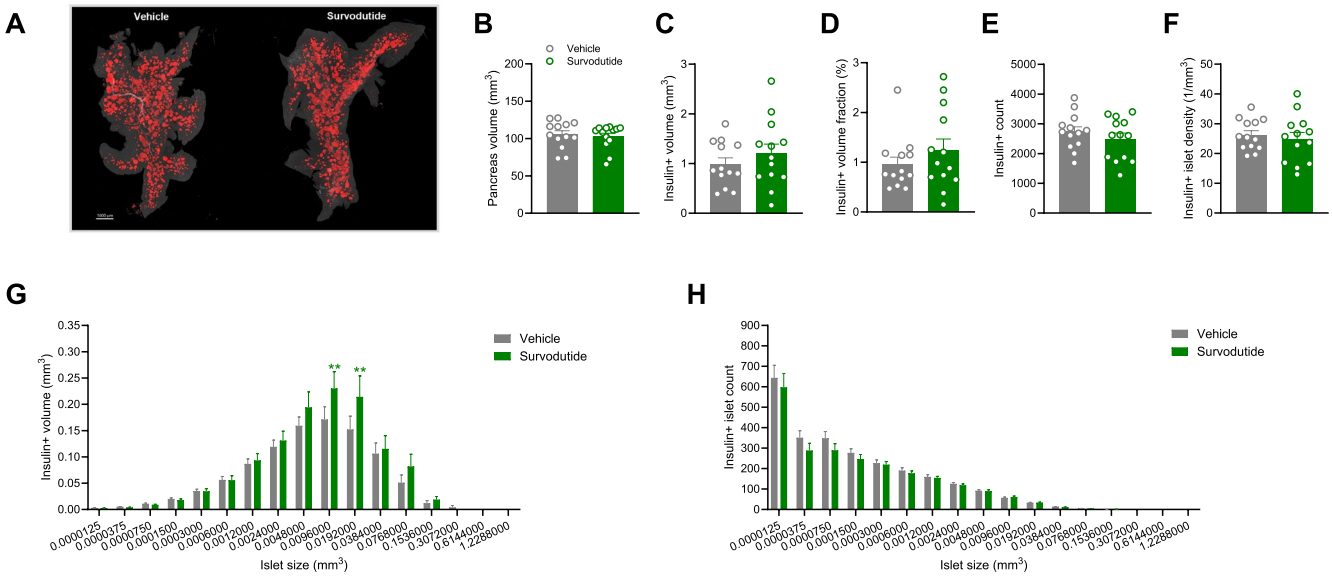


FIGURE 5 | Survodutide has minimal effect on pancreas and beta cell volumes in *db/db* UNx-ReninAAV mice as quantified by 3D whole-pancreas light-sheet fluorescence microscopy. (A) 3D light sheet fluorescence microscope (LSFM) scans are displayed as maximum intensity projections of pancreatic splenic lobes from the vehicle group and survodutide group with insulin signal (647 nm) in red and tissue anatomy (autofluorescence signal (561 nm) in grey). Scale bar, 1000 µm. Graphs show (B) total pancreas volume (mm^3) based on autofluorescence, (C) Insulin$^+$ volume (mm^3), (D) insulin$^+$ volume fraction (%, normalized to total pancreas volume), (E) total insulin$^+$ islet count, (F) insulin$^+$ islet density (islets/mm^3, normalized to pancreas volume). By categorizing islets of Langerhans by size, distribution plots display (G) Insulin$^+$ islet volumes (mm^3) and (H) Insulin$^+$ islet count for different islet sizes (0.0000125–1.2288 mm^3). Data presented as mean ± SEM ($n = 13$ per group). For single value data, Dunnett's test one-factor linear model used. For size distribution data, Dunnett's test on two-factor linear model with interaction used. **$p < 0.01$ compared to the Vehicle group.

14631326, 2026, 12, Downloaded from https://dom-pubs.onlinelibrary.wiley.com/doi/10.1111/dom.71387, Wiley Online Library on [05/11/2026]. See the Terms and Conditions (https://onlinelibrary.wiley.com/terms-and-conditions) on Wiley Online Library for rules of use; OA articles are governed by the applicable Creative Commons License

These biomarker changes are consistent with canonical effects of hepatic GCGR activation, reflecting increased ketogenesis and amino acid-dependent gluconeogenesis [34]. The improvement in glycemia observed with survodutide, despite acute GCGR activation, may be explained by the counterbalancing effects of GLP-1R signalling. Survodutide is more potent at the human GLP-1R (EC_{50}, 1 nM) than the human GCGR (EC_{50}, 8.3 nM) [19]. Furthermore, chronic GCGR activation promotes increased energy expenditure contributing to weight loss [19], which ultimately also improves hyperglycemia.

GLP-1R agonists have been shown to have nephroprotective effects in multiple preclinical [27, 35, 36] and clinical [11, 18, 37, 38] studies. However, it is presently unclear whether these effects are direct or secondary to its metabolic effects. The mode of action underlying the therapeutic effects of GLP-1R in DKD is incompletely understood and may likely be determined by both extra- and intrarenal actions [11, 39, 40]. In agreement with findings in DKD patients, semaglutide has been reported to improve hypertension, hyperglycemia, albuminuria and glomerulosclerosis in *db/db* UNx-ReninAAV mice [27]. In comparison, the sodium-glucose co-transporter-2 (SGLT2) inhibitor empagliflozin robustly reduced hyperglycemia without influencing hypertension and kidney histopathology in the model [22, 23, 41]. This implies that stimulating GLP-1R function improves kidney outcomes in *db/db* UNx-ReninAAV mice regardless of antihyperglycemic effects.

Survodutide increased plasma renin levels in *db/db* UNx-ReninAAV mice; however, it should be emphasized that kidney pathology in this model is independent of intrarenal renin expression, as renin overexpression is driven by a liver-specific promoter [23, 41]. As semaglutide has previously been reported to robustly improve hypertension in *db/db* UNx-ReninAAV mice while concomitantly increasing renin mRNA expression in the kidney [27], the renal renin signal appears unlikely to reflect activation of the renin-angiotensin-aldosterone system. Both semaglutide and liraglutide have been shown to increase renin mRNA expression in the renal vasculature, potentially contributing to GLP-1R-mediated angiogenesis and glomerular repair mechanisms [42, 43]. Supporting this concept, GLP-1R agonists promote vasodilation and increase intrarenal blood flow, possibly mediated by GLP-1Rs expressed in renal vasculature [44, 45]. Given that antihypertensive treatment intervention, using ACE inhibitors, has consistently been shown to alleviate kidney disease in the model [22, 23, 27, 41], this further supports that vasodilatory effects could play an important role in the nephroprotective effects of GLP-1R activation.

Despite GCGR expression in the nephron, tubules and collecting duct [13], its precise physiological role remains incompletely understood. The postprandial increase in glomerular filtration rate has been proposed to involve glucagon signalling, potentially reflecting a transient response that facilitates urea clearance associated with increased amino acid metabolism [46]. Notably, renal *GCGR* expression is downregulated in CKD patients [14, 15, 47] and shows a positive correlation with estimated eGFR in patients with DKD [16]. Supporting a functional role, *Gcgr-deficient* mice exhibit impaired kidney function, including albuminuria, polyuria, hyperaminoacidemia and hypertension [17]. Furthermore, *Gcgr* knockdown exacerbates glomerulosclerosis, tubulointerstitial fibrosis and inflammation in *db/db* mice and a mouse model of unilateral ureteral obstruction [47]. Survodutide markedly reduced renal F4/80 expression in *db/db* UNx-ReninAAV mice, indicative of anti-inflammatory activity. It has been speculated that reduced albuminuria following treatment with cotadutide, a GCGR/GLP-1R dual agonist, in DKD patients could be secondary to protective GCGR-mediated metabolic action at the tubular level [18]. Supporting this, the dual GLP-1R and GCGR agonist 1907-B improved glomerulosclerosis and tubulointerstitial fibrosis and reduced blood urea nitrogen and serum creatinine in *db/db* mice, even with *Glp1r* knockdown. Interestingly, glucagon alone reduced blood urea nitrogen, serum creatinine, glomerulosclerosis and tubulointerstitial fibrosis comparably to 1907-B. It should be noted that 1907-B has a 557-fold higher potency for the GLP-1R (EC_{50}, 0.08 nM) than GCGR (EC_{50}, 49.08 nM) [47], hence being more biased at the GLP-1R than survodutide.

Glomerular and tubular effects of GCGR activation, including enhanced natriuresis, may modulate renal hemodynamics and potentially attenuate glomerular hyperfiltration [17]. Thus, the GCGR component of survodutide may contribute to the renoprotective effects observed in the *db/db* UNx-ReninAAV mouse model, although its specific contribution cannot be established from the present study. Indeed, the role of GCGR signalling in DKD remains incompletely resolved, with findings from pharmacological studies being contradictory. For example, prolonged exposure to native glucagon has been associated with exacerbated kidney injury in a combined UNx, high-fat diet- and streptozotocin-induced mouse model of DKD [48], whereas long-acting dual GCGR/GLP-1R agonism differs fundamentally in its pharmacological and metabolic profile, including reductions in endogenous glucagon levels [19]. These observations suggest that the renal effects of GCGR activation are context dependent, varying with the underlying renal phenotype, duration of treatment and magnitude and temporal profile of GCGR activation. Accordingly, further studies using receptor-selective agonists and tissue-specific *Glp1r* and *Gcgr* knock-out models are required to define the specific contribution of GCGR signalling to the nephroprotective effects of survodutide.

Survodutide promotes weight loss through dual mechanisms, reduced food intake mediated by GLP-1R and increased energy expenditure mediated by GCGR, leading to greater weight reduction compared with GLP-1R agonist monotherapy [19, 49]. In agreement, survodutide markedly attenuated weight gain in *db/db* UNx-ReninAAV mice, which may have contributed, directly or indirectly, to the improved renal outcomes in the model. Mediation analyses from the LEADER and SUSTAIN 6 trials showed that body weight reduction contributed minimally to renoprotection with liraglutide and semaglutide, respectively. In contrast, HbA1c and systolic blood pressure accounted for a greater proportion of the renoprotective effect, while diastolic blood pressure had negligible impact [50]. Although blood pressure was not monitored in the present study, survodutide has been demonstrated to exert antihypertensive effects in clinical trials for obesity and type 2 diabetes [51, 52], with semaglutide previously shown to reduce blood pressure in *db/db* UNx-ReninAAV mice [27]. Survodutide also reduced HbA1c levels in *db/db* UNx-ReninAAV mice, consistent with findings in type 2 diabetes patients [53]. Although

14631326, 2026, 12, Downloaded from https://dom-pubs.onlinelibrary.wiley.com/doi/10.1111/dom.71387, Wiley Online Library on [05/11/2026]. See the Terms and Conditions (https://onlinelibrary.wiley.com/terms-and-conditions) on Wiley Online Library for rules of use; OA articles are governed by the applicable Creative Commons License

total β-cell volume was unchanged in *db/db* UNx-ReninAAV mice, survodutide modestly increased the volume of mid-sized insulin-positive islets. This finding is consistent with prior reports showing increased β-cell mass following GLP-1R agonist or SGLT2 inhibitor treatment in rodent models of diabetes, an effect attributed to preservation of β-cell integrity or delayed β-cell loss rather than enhanced β-cell proliferation [54–58]. Survodutide may therefore alleviate β-cell stress through improved glycemic control, reducing glucotoxicity and insulin demand, which could contribute to preservation of mid-sized insulin islets in *db/db* UNx-ReninAAV mice. As improvements in glycemic control and blood pressure are not solely attributable to weight loss and only partially account for the observed renoprotection, GLP-1R-mediated kidney benefits appear to be, at least in part, independent of weight loss.

Beyond reducing kidney and glomerular hypertrophy, survodutide increased whole-glomerular sphericity, consistent with a more regular and preserved glomerular morphology. Glomerular sphericity or circularity progressively declines with increasing CKD severity and has been identified as an independent predictor of disease progression [30, 31]. Moreover, experimental podocyte injury has been associated with loss of glomerular sphericity [59], supporting a potential link between glomerular geometry and podocyte structural integrity. Consistent with this concept, semaglutide has previously been shown to preserve podocyte filtration slit density in *db/db* UNx-ReninAAV mice [27]. Thus, the increased sphericity of podocin-positive glomeruli following survodutide treatment may reflect preservation or restoration of glomerular architecture, potentially contributing to the attenuation of severe proteinuria and advanced glomerulosclerosis in the model.

The therapeutic landscape of DKD has expanded substantially with SGLT2 inhibitors and GLP-1R agonists, which confer complementary cardiorenal protection. SGLT2 inhibitors, including empagliflozin and canagliflozin, exert kidney-protective effects in part by restoring tubuloglomerular feedback and reducing intraglomerular pressure, thereby lowering the risk of kidney disease progression and cardiovascular events [60–62]. In comparison, GLP-1R agonists, including semaglutide, provide broad systemic metabolic benefits, including improved glycaemic control and weight reduction, while also reducing major kidney disease events and attenuating eGFR decline in patients with DKD [11, 63]. Survodutide may extend this therapeutic paradigm by combining GLP-1R and GCGR agonism, thereby integrating effects on glycaemic control, energy intake, body weight and energy expenditure. Consistent with this profile, substantial and sustained weight loss has been demonstrated with survodutide in clinical obesity trials [51, 64]. In the present hypertension-accelerated DKD model, survodutide improved body weight, albuminuria and kidney histopathological endpoints within 10 weeks, indicating a rapid and broad therapeutic response. However, the onset and magnitude of these effects were not directly compared with those of SGLT2 inhibitors or selective GLP-1R agonists. Thus, whether dual GLP-1R/GCGR agonism confers incremental kidney protection beyond established therapies remains to be established in head-to-head preclinical and clinical studies. Moreover, although our findings provide preclinical evidence supporting a nephroprotective potential of survodutide, the kidney benefits have yet to be established clinically. A dedicated phase 2 trial (ARTIST-CKD; #NCT07206290, ClinicalTrials.gov) is currently evaluating the effects of survodutide on albuminuria in individuals with CKD and a CV safety phase 3 trial (SYNCHRONIZE-CVOT; # NCT06077864, ClinicalTrials.gov) investigates renal outcome and biomarkers as secondary endpoints.

The present study has several limitations. First, the hypertension-accelerated DKD model exhibits glomerular hyperfiltration rather than progressive GFR decline and does not develop prominent tubulointerstitial fibrosis [22], limiting its ability to recapitulate the functional decline and advanced tubulointerstitial pathology characteristic of progressive human DKD. Second, given the hypertensive phenotype of the model, blood pressure monitoring would have been valuable to distinguish blood pressure-dependent from independent effects of survodutide. Third, the absence of mediation analyses precludes determination of the extent to which the nephroprotective effects of survodutide are independent of weight loss and associated metabolic improvements. Fourth, although only female mice were studied, previous work indicates that male and female *db/db* UNx mice exhibit broadly similar progression of diabetes and major features of DKD, including albuminuria and renal and glomerular hypertrophy [25]. However, sex-dependent differences in renal pathology and treatment response cannot be entirely excluded and confirmation of the nephroprotective effects of survodutide in male *db/db* UNx-ReninAAV mice will be important to establish the generalizability of these findings across sexes. Finally, inclusion of additional comparator groups, such as *db/db* UNx and *db/db* mice, would further delineate the metabolic and renal effects of survodutide across different stages and severities of diabetic kidney injury.

5 | Conclusion

In conclusion, survodutide markedly ameliorates hallmarks of kidney disease and type 2 diabetes in the *db/db* UNx-ReninAAV mouse model of advanced DKD. Further studies are required to elucidate the precise mode of action of survodutide; however, the potential synergistic interplay between GLP-1R and GCGR activation suggests that survodutide may offer a promising and unique therapeutic strategy for patients with DKD and other forms of CKD.

Author Contributions

Conceived and designed the experiments: T.K., L.T., M.O., M.C. and H.H.H. Performed the experiments: L.T., M.H., R.A. and B.B. Analysed and interpreted the data: H.H.H., L.T., M.O., J.P., M.H., T.L., A.H., K.A. and W.R. Wrote the manuscript: H.H.H., A.H., T.K. and R.A.

Acknowledgements

The authors would like to acknowledge skilled assistance by Helene Dyhr, Bianca Olsen, Neringa Zitkuke and Sabrina Krarup. We are also grateful to Jens Borghardt for discussions regarding human dose estimation.

Funding

The study was supported and funded by Boehringer Ingelheim.

14631326, 2026, 12, Downloaded from https://dom-pubs.onlinelibrary.wiley.com/doi/10.1111/dom.71387, Wiley Online Library on [05/11/2026]. See the Terms and Conditions (https://onlinelibrary.wiley.com/terms-and-conditions) on Wiley Online Library for rules of use; OA articles are governed by the applicable Creative Commons License

Conflicts of Interest

A.H., L.T., M.O., M.H., K.A., M.C., and H.H.H. are employed by Gubra A/S; J.P. was employed by Gubra at the time of study and is now employed at Vibraint ApS. All are shareholders in Gubra A/S. Robert Augustin R.A., B.B., W.R. and T.K. are employed by Boehringer Ingelheim. The authors meet criteria for authorship as recommended by the International Committee of Medical Journal Editors (ICMJE) as supported by Good Publication Practice (GPP) guidelines. The authors did not receive payment related to the development of the presentation. Kayleigh Walker, PhD, of Envision Ignite, an Envision Medical Communications agency, a part of Envision Pharma Group, provided writing support, which was contracted and funded by Boehringer Ingelheim. Boehringer Ingelheim was given the opportunity to review the presentation for medical and scientific accuracy as well as intellectual property considerations. Survodutide is licensed to Boehringer Ingelheim from Zealand Pharma.

Data Availability Statement

Supplementary video material is openly available on Figshare (https://doi.org/10.6084/m9.figshare.31850719).

Peer Review

The peer review history for this article is available at https://www.webofscience.com/api/gateway/wos/peer-review/10.1111/dom.71387.

References

1. N. R. Hill, S. T. Fatoba, J. L. Oke, et al., "Global Prevalence of Chronic Kidney Disease - A Systematic Review and Meta-Analysis," *PLoS One* 11 (2016): e0158765.

2. V. Harjutsalo and P. H. Groop, "Epidemiology and Risk Factors for Diabetic Kidney Disease," *Advances in Chronic Kidney Disease* 21 (2014): 260–266.

3. S. Hamada and M. C. Gulliford, "Multiple Risk Factor Control, Mortality and Cardiovascular Events in Type 2 Diabetes and Chronic Kidney Disease: A Population-Based Cohort Study," *BMJ Open* 8 (2018): e019950.

4. M. C. Thomas, M. Brownlee, K. Susztak, et al., "Diabetic Kidney Disease," *Nature Reviews. Disease Primers* 1 (2015): 15018.

5. F. Persson, R. Borg, and P. Rossing, "A Narrative Review of New Treatment Options for Chronic Kidney Disease in Type 2 Diabetes," *Annals of Translational Medicine* 9 (2021): 716.

6. S. P. Marso, G. H. Daniels, K. Brown-Frandsen, et al., "Liraglutide and Cardiovascular Outcomes in Type 2 Diabetes," *New England Journal of Medicine* 375 (2016): 311–322.

7. S. P. Marso, S. C. Bain, A. Consoli, et al., "Semaglutide and Cardiovascular Outcomes in Patients With Type 2 Diabetes," *New England Journal of Medicine* 375 (2016): 1834–1844.

8. K. R. Tuttle, M. C. Lakshmanan, B. Rayner, et al., "Dulaglutide Versus Insulin Glargine in Patients With Type 2 Diabetes and Moderate-To-Severe Chronic Kidney Disease (AWARD-7): A Multicentre, Open-Label, Randomised Trial," *Lancet Diabetes and Endocrinology* 6 (2018): 605–617.

9. S. V. Badve, A. Bilal, M. M. Y. Lee, et al., "Effects of GLP-1 Receptor Agonists on Kidney and Cardiovascular Disease Outcomes: A Meta-Analysis of Randomised Controlled Trials," *Lancet Diabetes and Endocrinology* 13 (2025): 15–28.

10. A. M. Shaman, S. C. Bain, G. L. Bakris, et al., "Effect of the Glucagon-Like Peptide-1 Receptor Agonists Semaglutide and Liraglutide on Kidney Outcomes in Patients With Type 2 Diabetes: Pooled Analysis of SUSTAIN 6 and LEADER," *Circulation* 145 (2022): 575–585.

11. V. Perkovic, K. R. Tuttle, P. Rossing, et al., "Effects of Semaglutide on Chronic Kidney Disease in Patients With Type 2 Diabetes," *New England Journal of Medicine* 391 (2024): 109–121.

12. L. Bankir, N. Bouby, B. Blondeau, and G. Crambert, "Glucagon Actions on the Kidney Revisited: Possible Role in Potassium Homeostasis," *American Journal of Physiology. Renal Physiology* 311 (2016): F469–F486.

13. A. B. Bomholt, C. D. Johansen, J. B. Christensen, et al., "Evaluation of Commercially Available Glucagon Receptor Antibodies and Glucagon Receptor Expression," *Communications Biology* 5 (2022): 1278.

14. P. Perco, W. Ju, J. Kerschbaum, et al., "Identification of Dicarbonyl and L-Xylulose Reductase as a Therapeutic Target in Human Chronic Kidney Disease," *JCI Insight* 4 (2019): e128120.

15. P. C. Grayson, S. Eddy, J. N. Taroni, et al., "Metabolic Pathways and Immunometabolism in Rare Kidney Diseases," *Annals of the Rheumatic Diseases* 77 (2018): 1227–1234.

16. Y. Fan, Z. Yi, V. D. D'Agati, et al., "Comparison of Kidney Transcriptomic Profiles of Early and Advanced Diabetic Nephropathy Reveals Potential New Mechanisms for Disease Progression," *Diabetes* 68 (2019): 2301–2314.

17. M. Y. Wang, Z. Zhang, S. Zhao, et al., "Downregulation of the Kidney Glucagon Receptor, Essential for Renal Function and Systemic Homeostasis, Contributes to Chronic Kidney Disease," *Cell Metabolism* 36 (2024): 575–597.e7.

18. V. Selvarajah, D. Robertson, L. Hansen, et al., "A Randomized Phase 2b Trial Examined the Effects of the Glucagon-Like Peptide-1 and Glucagon Receptor Agonist Cotadutide on Kidney Outcomes in Patients With Diabetic Kidney Disease," *Kidney International* 106 (2024): 1170–1180.

19. T. Zimmermann, L. Thomas, T. Baader-Pagler, et al., "BI 456906: Discovery and Preclinical Pharmacology of a Novel GCGR/GLP-1R Dual Agonist With Robust Anti-Obesity Efficacy," *Molecular Metabolism* 66 (2022): 101633.

20. S. Wharton, C. W. le Roux, M. N. Kosiborod, et al., "Survodutide for Treatment of Obesity: Rationale and Design of Two Randomized Phase 3 Clinical Trials (SYNCHRONIZE-1 and -2)," *Obesity* 33 (2024): 67–77.

21. A. J. Sanyal, P. Bedossa, M. Fraessdorf, et al., "A Phase 2 Randomized Trial of Survodutide in MASH and Fibrosis," *New England Journal of Medicine* 391 (2024): 311–319.

22. M. V. Østergaard, T. Secher, M. Christensen, et al., "Therapeutic Effects of Lisinopril and Empagliflozin in a Mouse Model of Hypertension-Accelerated Diabetic Kidney Disease," *American Journal of Physiology. Renal Physiology* 321 (2021): F149–F161.

23. S. M. Harlan, K. M. Heinz-Taheny, J. M. Sullivan, et al., "Progressive Renal Disease Established by Renin-Coding Adeno-Associated Virus-Driven Hypertension in Diverse Diabetic Models," *Journal of the American Society of Nephrology* 29 (2018): 477–491.

24. H. Ninomiya, T. Inomata, and K. Ogihara, "Obstructive Uropathy and Hydronephrosis in Male KK-Ay Mice: A Report of Cases," *Journal of Veterinary Medical Science* 61 (1999): 53–57.

25. F. E. Sembach, L. N. Fink, T. Johansen, et al., "Impact of Sex on Diabetic Nephropathy and the Renal Transcriptome in UNx Db/Db C57BLKS Mice," *Physiological Reports* 7 (2019): e14333.

26. D. A. Springer, M. Allen, V. Hoffman, et al., "Investigation and Identification of Etiologies Involved in the Development of Acquired Hydronephrosis in Aged Laboratory Mice With the Use of High-Frequency Ultrasound Imaging," *Pathobiology of Aging & Age-Related Diseases* 4 (2014): 24932.

27. L. S. Dalbøge, M. Christensen, M. R. Madsen, et al., "Nephroprotective Effects of Semaglutide as Mono- and Combination Treatment With Lisinopril in a Mouse Model of Hypertension-Accelerated Diabetic Kidney Disease," *Biomedicine* 10 (2022): 1661.

14631326, 2026, 12, Downloaded from https://dom-pubs.onlinelibrary.wiley.com/doi/10.1111/dom.71387, Wiley Online Library on [05/11/2026]. See the Terms and Conditions (https://onlinelibrary.wiley.com/terms-and-conditions) on Wiley Online Library for rules of use; OA articles are governed by the applicable Creative Commons License

28. M. V. Østergaard, F. E. Sembach, J. L. Skytte, et al., "Automated Image Analyses of Glomerular Hypertrophy in a Mouse Model of Diabetic Nephropathy," *Kidney360* 1 (2020): 469–479.

29. N. Wang, Z. Lu, W. Zhang, Y. Bai, D. Pei, and L. Li, "Serum Cystatin C Trajectory Is a Marker Associated With Diabetic Kidney Disease," *Frontiers in Endocrinology* 13 (2022): 824279.

30. Q. He, J. Li, T. Guan, et al., "GloPath: An Entity-Centric Foundation Model for Glomerular Lesion Assessment and Clinicopathological Insights," *Advanced Science* 13 (2026): e20580.

31. D. L. Hölscher, N. Bouteldja, M. Joodaki, et al., "Next-Generation Morphometry for Pathomics-Data Mining in Histopathology," *Nature Communications* 14 (2023): 470.

32. L. Thomas, E. Martel, W. Rist, et al., "The Dual GCGR/GLP-1R Agonist Survodutide: Biomarkers and Pharmacological Profiling for Clinical Candidate Selection," *Diabetes, Obesity & Metabolism* 26 (2024): 2368–2378.

33. H. H. Hansen, G. Hansen, T. Secher, et al., "Animal Models of Type 2 Diabetes, Obesity and Nonalcoholic Steatohepatitis – Clinical Translatability and Applicability in Preclinical Drug Development," in *Translational Research Methods in Diabetes, Obesity, and Nonalcoholic Fatty Liver Disease: A Focus on Early Phase Clinical Drug Development* (Springer, 2019), 369–403.

34. N. J. Wewer Albrechtsen, J. J. Holst, A. D. Cherrington, et al., "100 Years of Glucagon and 100 More," *Diabetologia* 66 (2023): 1378–1394.

35. C. Wang, L. Li, S. Liu, et al., "GLP-1 Receptor Agonist Ameliorates Obesity-Induced Chronic Kidney Injury via Restoring Renal Metabolism Homeostasis," *PLoS One* 13 (2018): e0193473.

36. R. Li, D. She, Z. Ye, et al., "Glucagon-Like Peptide 1 Receptor Agonist Improves Renal Tubular Damage in Mice With Diabetic Kidney Disease," *Diabetes, Metabolic Syndrome and Obesity* 15 (2022): 1331–1345.

37. H. C. Gerstein, H. M. Colhoun, G. R. Dagenais, et al., "Dulaglutide and Cardiovascular Outcomes in Type 2 Diabetes (REWIND): A Double-Blind, Randomised Placebo-Controlled Trial," *Lancet* 394 (2019): 121–130.

38. S. P. Marso, G. H. Daniels, K. Brown-Frandsen, et al., "Liraglutide and Cardiovascular Outcomes in Type 2 Diabetes," *New England Journal of Medicine* 375 (2016): 101.

39. R. Z. Alicic, E. J. Cox, J. J. Neumiller, and K. R. Tuttle, "Incretin Drugs in Diabetic Kidney Disease: Biological Mechanisms and Clinical Evidence," *Nature Reviews Nephrology* 17, no. 4 (2021): 227–244.

40. E. D. Michos, G. L. Bakris, H. W. Rodbard, and K. R. Tuttle, "Glucagon-Like Peptide-1 Receptor Agonists in Diabetic Kidney Disease: A Review of Their Kidney and Heart Protection," *American Journal of Preventive Cardiology* 14 (2023): 100502.

41. S. M. Harlan, K. M. Heinz-Taheny, J. M. Overstreet, M. D. Breyer, R. C. Harris, and J. G. Heuer, "Pathological and Transcriptome Changes in the Renin AAV Db/Db uNx Model of Advanced Diabetic Kidney Disease Exhibit Features of Human Disease," *Toxicologic Pathology* 46 (2018): 991–998.

42. K. D. Bjørnholm, M. E. Ougaard, G. F. Skovsted, L. B. Knudsen, and C. Pyke, "Activation of the Renal GLP-1R Leads to Expression of Ren1 in the Renal Vascular Tree," *Endocrinology, Diabetes & Metabolism* 4 (2021): e00234.

43. R. Ariel Gomez and M. L. S. Sequeira-Lopez, "Renin Cells in Homeostasis, Regeneration and Immune Defence Mechanisms," *Nature Reviews Nephrology* 14 (2018): 231–245.

44. A. V. R. Hviid and C. M. Sørensen, "Glucagon-Like Peptide-1 Receptors in the Kidney: Impact on Renal Autoregulation," *American Journal of Physiology. Renal Physiology* 318 (2020): F443–F454.

45. E. P. Jensen, S. S. Poulsen, H. Kissow, et al., "Activation of GLP-1 Receptors on Vascular Smooth Muscle Cells Reduces the Autoregulatory Response in Afferent Arterioles and Increases Renal Blood Flow," *American Journal of Physiology. Renal Physiology* 308 (2015): F867–F877.

46. L. Bankir, N. Bouby, R. C. Speth, G. Velho, and G. Crambert, "Glucagon Revisited: Coordinated Actions on the Liver and Kidney," *Diabetes Research and Clinical Practice* 146 (2018): 119–129.

47. Q. Zhao, J. Dong, H. Liu, et al., "Design and Discovery of a Highly Potent Ultralong-Acting GLP-1 and Glucagon Co-Agonist for Attenuating Renal Fibrosis," *Acta Pharmaceutica Sinica B* 14 (2024): 1283–1301.

48. X. Liu, J. Chen, S. Gu, et al., "Prolonged Glucagon Exposure Rewires Lipid Oxidation and Drives Diabetic Kidney Disease Progression," *Nature Communications* 16 (2025): 8561.

49. F. Long, T. D. Challa, V. Efthymiou, et al., "Hepatic GCGR Is Required for the Superior Weight Loss and Metabolic Effects of a Structurally Related Analogue of the Dual GCGR/GLP-1R Agonist Survodutide in Mice," *Diabetes, Obesity and Metabolism* 28 (2025): 2437-.

50. J. F. E. Mann, J. B. Buse, T. Idorn, et al., "Potential Kidney Protection With Liraglutide and Semaglutide: Exploratory Mediation Analysis," *Diabetes, Obesity & Metabolism* 23 (2021): 2058–2066.

51. C. W. le Roux, O. Steen, K. J. Lucas, E. Startseva, A. Unseld, and A. M. Hennige, "Glucagon and GLP-1 Receptor Dual Agonist Survodutide for Obesity: A Randomised, Double-Blind, Placebo-Controlled, Dose-Finding Phase 2 Trial," *Lancet Diabetes and Endocrinology* 12 (2024): 162–173.

52. C. W. le Roux, O. Steen, E. L. Ekinci, et al., "Survodutide, a Glucagon Receptor/Glucagon-Like Peptide-1 Receptor Dual Agonist, Improves Blood Pressure in Adults With Obesity: A Post Hoc Analysis From a Randomized, Placebo-Controlled, Dose-Finding, Phase 2 Trial," *Diabetes, Obesity and Metabolism* 27 (2025): 993–996.

53. M. Blüher, J. Rosenstock, J. Hoefler, R. Manuel, and A. M. Hennige, "Dose-Response Effects on HbA1c and Bodyweight Reduction of Survodutide, a Dual Glucagon/GLP-1 Receptor Agonist, Compared With Placebo and Open-Label Semaglutide in People With Type 2 Diabetes: A Randomised Clinical Trial," *Diabetologia* 67 (2024): 470–482.

54. H. H. Hansen, J. Jelsing, C. F. Hansen, et al., "The Sodium Glucose Cotransporter Type 2 Inhibitor Empagliflozin Preserves β-Cell Mass and Restores Glucose Homeostasis in the Male Zucker Diabetic Fatty Rat," *Journal of Pharmacology and Experimental Therapeutics* 350 (2014): 657–664.

55. J. Sturis, C. F. Gotfredsen, J. Rømer, et al., "GLP-1 Derivative Liraglutide in Rats With Beta-Cell Deficiencies: Influence of Metabolic State on Beta-Cell Mass Dynamics," *British Journal of Pharmacology* 140 (2003): 123–132.

56. N. Vrang, J. Jelsing, L. Simonsen, et al., "The Effects of 13 Wk of Liraglutide Treatment on Endocrine and Exocrine Pancreas in Male and Female ZDF Rats: A Quantitative and Qualitative Analysis Revealing no Evidence of Drug-Induced Pancreatitis," *American Journal of Physiology. Endocrinology and Metabolism* 303 (2012): E253–E264.

57. S. Cernea and R. A. Z. Itamar, "Therapy in the Early Stage: Incretins," *Diabetes Care* 34 (2011): S264–S271.

58. T. Kimura, H. Kaneto, M. Shimoda, et al., "Protective Effects of Pioglitazone and/or Liraglutide on Pancreatic β-Cells in Db/Db Mice: Comparison of Their Effects Between in an Early and Advanced Stage of Diabetes," *Molecular and Cellular Endocrinology* 400 (2015): 78–89.

59. M. N. Basso, M. Barua, R. John, and A. Khademi, "Explainable Biomarkers for Automated Glomerular and Patient-Level Disease Classification," *Kidney360* 3 (2021): 534–545.

60. W. G. Herrington, N. Staplin, C. Wanner, et al., "Empagliflozin in Patients With Chronic Kidney Disease," *New England Journal of Medicine* 388 (2023): 117–127.

61. V. Perkovic, M. J. Jardine, B. Neal, et al., "Canagliflozin and Renal Outcomes in Type 2 Diabetes and Nephropathy," *New England Journal of Medicine* 380 (2019): 2295–2306.

14631326, 2026, 12, Downloaded from https://dom-pubs.onlinelibrary.wiley.com/doi/10.1111/dom.71387, Wiley Online Library on [05/11/2026]. See the Terms and Conditions (https://onlinelibrary.wiley.com/terms-and-conditions) on Wiley Online Library for rules of use; OA articles are governed by the applicable Creative Commons License

62. R. A. DeFronzo, W. B. Reeves, and A. S. Awad, "Pathophysiology of Diabetic Kidney Disease: Impact of SGLT2 Inhibitors," *Nature Reviews. Nephrology* 17 (2021): 319–334.

63. R. Z. Alicic, J. J. Neumiller, and K. R. Tuttle, "GLP-1 Receptor Agonists and Next-Generation Metabolic Hormone Therapies in Chronic Kidney Disease," *Nature Reviews. Nephrology* 22 (2026): 265–282.

64. C. W. le Roux, S. Wharton, E. Startseva, et al., "Survodutide Once Weekly for the Treatment of Adults With Obesity," *New England Journal of Medicine* 392 (2026): 776–787.

Supporting Information

Additional supporting information can be found online in the Supporting Information section. **Data S1:** 3D whole-organ imaging analysis. **Figure S1:** Randomization and stratification. *db/db* Renin AAV-UNx mice were randomized and stratified to treatment groups according to (A) body weight, (B) blood glucose and (C) urine ACR. Data presented as mean ± SEM. Dunnett's test one-factor linear model used. No significant difference ($p < 0.05$) were observed between groups. **Figure S2:** Human translational dose-prediction for survodutide. (A) Translational dose-prediction workflow. Subchronic pharmacodynamic (PD) studies in *db/db* and diet-induced obesity (DIO) mice, respectively, defined the efficacious exposure (7.5 nmol/kg, s.c., q.d.; HbA1c and body-weight loss, see mouse data in Panel B). The corresponding average steady-state concentration ($C_{ave,ss} \approx 109$ nM), supported by the low mouse peak/trough ratio (1.03), was set as the human steady-state target. Predicted human pharmacokinetic (PK) parameters [apparent clearance (CL/F) 0.000768 L/h/kg; bioavailability (F) 60%, volume of distribution at steady state (V_{ss}) 0.108 L/kg; half-life $t_{½}$ 62 h; mean residence time (MRT) 234 h], were applied to predict the human efficacious dose range. (B) In vivo efficacy in *db/db* and DIO mice. *Left panel*: female *db/db* mice treated for 4 weeks with survodutide (7.5 and 10 nmol/kg s.c., q.d.); change in HbA1c from baseline. *Right panel*: DIO mice (3 months on high-fat diet) treated for 4 weeks (7.5 and 10 nmol/kg, s.c., q.d.). Data are shown as mean ± S.E.M. ($n = 10$ per group). *$p < 0.05$, ***$p < 0.001$. (C) Exemplary simulated human steady-state PK profile at 6.0 mg, s.c. once weekly ($C_{max,ss}$ 142 nM, $C_{ave,ss}$ 109 nM [target], $C_{min,ss}$ 79 nM; peak/trough 1.80). For the underlying mouse PK data, see Zimmermann *et al.*, Mol. Metab. 66:101633, 2022. **Figure S3:** Liver weight following 10 weeks of survodutide treatment in *db/db* Renin AAV-UNx mice. Liver weight after treatment with vehicle ($n = 15$) and survodutide ($n = 15$). Data presented as mean ± SEM. Dunnett's test one-factor linear model used. ***$p < 0.001$ compared to vehicle control. **Figure S4:** Plasma amino acid levels following 10 weeks of survodutide treatment in *db/db* Renin AAV-UNx mice. Plasma amino acid concentrations after treatment with vehicle ($n = 12$) or survodutide ($n = 6$). Unpaired *t*-test used. *$p < 0.05$, **$p < 0.01$ compared to the vehicle group. **Figure S5:** Glomeruli sphericity distribution in *db/db* UNx-Renin AAV mice as quantified by 3D whole-kidney light-sheet fluorescence microscopy. Glomeruli generally exhibited high sphericity across treatment groups. Survodutide increased the sphericity of glomeruli with relatively high shape regularity. Sphericity analysis was performed in mice treated with vehicle ($n = 14$) or survodutide ($n = 15$). Each point represents the percentage of glomeruli per sample with a given sphericity (0.01 intervals), where sphericity = 1.0 represents a perfect sphere.

14631326, 2026, 12, Downloaded from https://dom-pubs.onlinelibrary.wiley.com/doi/10.1111/dom.71387, Wiley Online Library on [05/11/2026]. See the Terms and Conditions (https://onlinelibrary.wiley.com/terms-and-conditions) on Wiley Online Library for rules of use; OA articles are governed by the applicable Creative Commons License